Langmuir

Article

pubs.acs.org/Langmuir

Triboelectricity: Macroscopic Charge Patterns Formed by Self-Arraying Ions on Polymer Surfaces

Thiago A. L. Burgo,[†] Telma R. D. Ducati,[†] Kelly R. Francisco,[†] Karl J. Clinckspoor,[†] Fernando Galembeck,*[,†,§] and Sergio E. Galembeck[¶]

[†]Institute of Chemistry, University of Campinas, Campinas SP, Brazil 13083-970

[§]National Nanotechnology Laboratory at the National Center for Energy and Materials Research, Campinas SP, Brazil 13083-970

[¶]Chemistry Department, University of São Paulo, Ribeirão Preto SP, Brazil 14040-901

Supporting Information

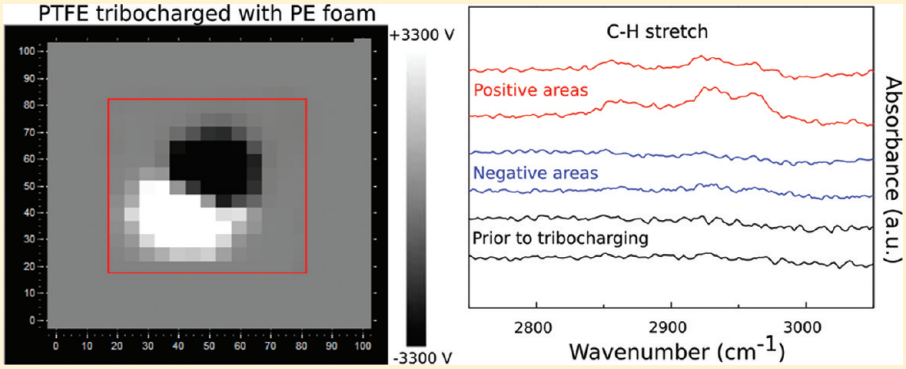

ABSTRACT: Tribocharged polymers display macroscopically patterned positive and negative domains, verifying the fractal geometry of electrostatic mosaics previously detected by electric probe microscopy. Excess charge on contacting polyethylene (PE) and polytetrafluoroethylene (PTFE) follows the triboelectric series but with one caveat: net charge is the arithmetic sum of patterned positive and negative charges, as opposed to the usual assumption of uniform but opposite signal charging on each surface. Extraction with *n*-hexane preferentially removes positive charges from PTFE, while 1,1-difluoroethane and ethanol largely remove both positive and negative charges. Using suitable analytical techniques (electron energy-loss spectral imaging, infrared microspectrophotometry and carbonization/colorimetry) and theoretical calculations, the positive species were identified as hydrocarbocations and the negative species were identified as fluorocarbanions. A comprehensive model is presented for PTFE tribocharging with PE: mechanochemical chain homolytic rupture is followed by electron transfer from hydrocarbon free radicals to the more electronegative fluorocarbon radicals. Polymer ions self-assemble according to Flory–Huggins theory, thus forming the experimentally observed macroscopic patterns. These results show that tribocharging can only be understood by considering the complex chemical events triggered by mechanical action, coupled to well-established physicochemical concepts. Patterned polymers can be cut and mounted to make macroscopic electrets and multipoles.

INTRODUCTION

Thales discovered contact electrification 25 centuries ago, and this topic has received attention from many important scientists over the past 200 years.[1] However, there is persistent controversy[2−6] concerning the nature of the species responsible for imparting charge to electrical insulators, in polymer−polymer or polymer−metal contacts.[7−10] Evidence in favor of electrons[11−17] or ions[18−26] as charge carriers has been presented by different groups in a debate that was much intensified during the past decade.

According to many authors, the outcome of contact electrification can be predicted using the triboelectric series which sums up experimental information on the positive or negative signal of charge found in a solid, following contact with any other solid. However, there is no accepted theoretical basis for the triboelectric series, and quantitative data are scarce. Indeed, even the position of different materials in the triboelectric series has been re-examined, from time to time.[27]

A recent publication[28] challenged the concept of triboelectric series, based on experiments made by contacting two surfaces of identical chemical composition, measuring the resulting electric charges and observing electrostatic potential mosaic patterns on these surfaces, by using Kelvin force microscopy. Terris et al.[29] and Knorr[30] had previously described related microscopy results, showing that surface scratching produces a bipolar or multipolar potential distribution. On the other hand, tribocharging can be sufficiently well-defined to allow macroscopic particle self-assembly.[31]

Received: March 23, 2012
Revised: April 19, 2012
Published: April 24, 2012

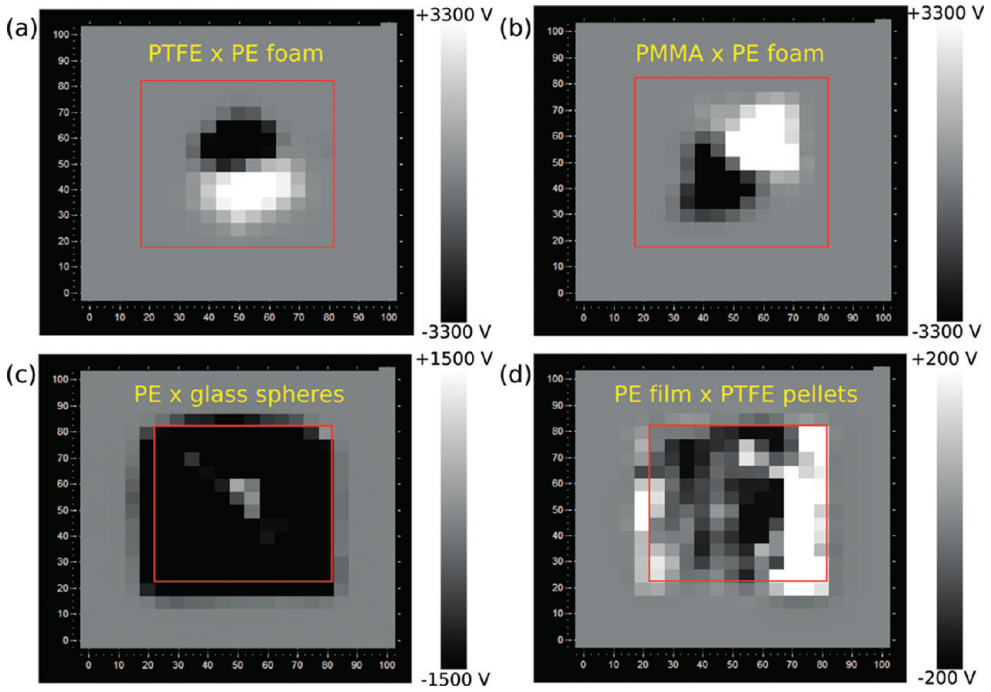

Figure 1. Macroscopic potential patterns obtained using two tribocharging techniques. (a) PTFE and (b) PMMA rubbed with PE foam disk. PE film abraded with (c) glass spheres and (d) PTFE pellets in a planetary mixer. Red squares indicate polymer area on each image and the *x*, *y* axes are in millimeters. Positive and negative domains covering many millimeters or centimeters are observed in every case. See also Supporting Information Figure S1.

Work done in the authors' laboratory over the past twelve years[24−26,32−37] showed electrostatic patterns on the surface of every dielectric solid examined, including carefully cleaned, nonscratched surfaces. In some cases, potential patterns could be explained by using microchemical data obtained by using analytical transmission electron microscopy (ESI-TEM) together with Kelvin microscopy: local excess of cations (or anions) creates domains with excess positive (or negative) charge.[33] However, in many other cases the species responsible for excess charge still could not be identified by this combination of techniques due either to the nature of the ionic species or to its low concentration. Direct evidence for the participation of ions derived from water—$[H(H_2O)_n]^+$, $[OH(H_2O)_n]^-$—was obtained, analogous to previous evidence for hydrophobic/nonpolar water interfaces[37,38] and helped to understand electrostatic charge build-up and dissipation in many experiments.[39] This result was further strengthened by the preparation of bulk water with steady excess charge, both positive and negative.[40]

Fractal dimensions of line or area features of electrostatic potential maps are often larger than fractal dimensions of the corresponding morphology features, showing that charge mobility is generally even lower than the mobility of surface molecules or macromolecular segments, especially in organic polymers. On the other hand, scale symmetry is a universal property of fractal objects, and it implies that potential and charge patterns should be found at any scale. The first experimental demonstration of the formation of macroscopic potential patterns in polyethylene[39] (PE) was recently published. The present paper shows for the first time that macroscopic patterns are obtained in many kinds of tribochemical experiments. Furthermore, experimental evidence is provided showing that tribocharges formed by shearing PE and polytetrafluoroethylene (PTFE) are selectively extracted by common solvents. We also show that positively and negatively charged species derive from PE and from PTFE, respectively. Finally, the reasons for macroscopic charge self-arraying into positive or negative domains and the factors for charge stability are discussed, based on Flory−Huggins theory for polymer solutions and on well-established ideas on the orientation of amphiphiles at interfaces.

EXPERIMENTAL SECTION

Polytetrafluoroethylene (PTFE), poly(methyl methacrylate (PMMA) and polyethylene (PE) were sheets sold for general use and immersed in ethanol for 2 h prior to tribocharging experiments. This is based on preliminary results showing that immersion in ethanol and a few other liquids largely eliminates static charges.

Two tribocharging procedures were used: (a) Square sheets (6 × 6 or 2 × 2 cm^2) of each polymer were supported on an aluminum holder mounted on a table-top balance and then rubbed with a disk of another polymer (φ = 25 mm or 10 mm) fixed on the chuck of a drilling machine, which was spun at 5000 rpm for 3 s. The pressure exerted by the spinning disk on the sample was adjusted to 1.5 ± 0.25 kPa, by measuring the force applied to the balance. (b) The polymer sample (6 cm × 6 cm) was mounted on top of an aluminum plate that laid on the horizontal table of a planetary lab shaker. Four grams of glass spheres (φ = 1 mm) or PTFE pellets (5 × 5 × 1 mm^3) were spread on top of the sample and the setup was shaken for 60 min, at 5 Hz reciprocating frequency and 10 mm amplitude.

The scanning apparatus for noncontact electric potential measurements and the controlling software were built by Optron (Campinas). Samples are held on a 10-mm-thick aluminum plate and scanned horizontally with a disk-shaped 5-mm-diameter Kelvin electrode connected to a voltmeter (model 347, Trek Inc.). This system can measure potentials within the ±3300 V range and, the spatial resolution (5 × 5 mm^2) is limited by the Kelvin electrode dimensions. The electrode moves in the *x*−*y* plane, 2 mm above the tested surface as recommended by the electrode manufacturer. Electrostatic potential scans started immediately after all samples had been abraded. Time allowed for the electrode equilibration on each pixel is 3 s. After

dx.doi.org/10.1021/la301228j | *Langmuir* 2012, 28, 7407−7416

potential measurements, polymers were placed within a Faraday cup for charge measurement using an electrometer (model 6514, Keithley Instruments).

Tribocharged PTFE surfaces were analyzed using three different techniques: infrared microreflectance (ATR/IR), pyrolysis, and electron-energy loss spectroscopy (EELS). Negative and positive areas were cut out from previously tribocharged samples using a grounded metal blade and ATR/IR spectra of a 50 μm^2 area were acquired with a Smiths IlluminatIR II instrument coupled to an Olympus BX51 microscope, using ZnSe windows, 64 scans and 4 cm^{-1} resolution. Pyrolysis experiments were done on tribocharged PTFE surfaces (2 × 2 cm^2) with a PE disk (φ = 10 mm) at 320 °C. EELS spectra and energy-filtered transmission electron microscopy images (EFTEM) were obtained from extracts of tribocharged domains using a Carl Zeiss CEM-902 transmission electron microscope. Elemental images were obtained using the three-window method and the energy-selecting slit was set at 303 eV for C, 544 eV for O, and 694 eV for F. The images were acquired using a Slow Scan CCD camera (Proscan) and processed in the iTEM Universal TEM Imaging Platform.

Simulation Methods. Evaluation of surface charge density on the samples follows the procedure described in previous papers.[26,39] Each pixel on the surface map is a square with 5 mm sides and this is further subdivided in a 500 × 500 pixel matrix, where virtual charges are placed. The electrostatic potential (V_T) measured 2 mm away from the matrix plane is generated by all charges (q_i) weighted by the distance r from the charge to the measuring point, and can be calculated, using a C++ code for equation of superposition principle defined as follows:

$$V_T = \sum_{i=1}^{n} V = \frac{1}{4\pi\varepsilon_0} \sum_{i=1}^{n} \frac{q_i}{r_i} \quad (1)$$

The number of excess charges per pixel is adjusted by trial and error, until the calculated and measured potentials match, within experimental error.

The standard free energies for hydrocarbon and fluorocarbon anion or cation formation from the respective free radicals were calculated by (U)B3LYP/6-31+G(d,p) computational model. Geometries were fully optimized and the vibrational frequencies were calculated. The calculations were made by *Gaussian09* software.[41]

RESULTS AND DISCUSSION

Every tribocharging experiment made in this laboratory led to nonuniformly charged polymer surfaces, forming macroscopic potential and charge patterns or mosaics. Figure 1 shows potential patterns recorded by scanning PTFE and PMMA surfaces that were previously tribocharged by rubbing with a spinning PE foam disk, under controlled pressure and speed.

Electrostatic potential on many pixels is in excess of ±3 kV, showing that the PTFE surface contains segregated positive and negative fixed charges arranged within macroscopic (positive or negative) domains in the millimeter−centimeter range, which is rather counterintuitive and is not expected within the conceptual framework of the triboelectric series. Charge surface concentration that produces 3 kV potential at a 2 mm electrode−sample distance is 254 charges/μm^2. This means that the average distance between ions accounting for excess local charge is in the 60 nm range. Assuming that the area occupied by an ion is in the 0.1−1 nm^2 range, the fraction of surface area occupied by the excess ions—those that account for excess charge in the macroscopic domains—is less than 0.03%, and the volume concentration of net excess charges in the surface layer is ca. 10^{-7} mol L^{-1}. At this low concentration, electrostatic repulsive interactions are very low, following the classical Debye−Hückel theory for electrolyte solutions.

Potential maps are also shown for PE films tribocharged with glass balls and PTFE pellets on top of the table of a planetary mixer. Again, nonuniform charging is observed: positive domains predominate on the PE surface scratched with PTFE, but they are scarce on PE that contacted glass balls. These experiments were repeated many times, and a set of maps obtained by abrading PTFE with PE foam or PE with PTFE is in Supporting Information Figure S1. The maps themselves are not reproducible in detail, but the patterns obtained are reproducible: tribocharged PTFE potential maps always show two large adjacent areas, one positive and the other negative. The overall charged area is larger than the area of the spinning disk: the diameter of the latter is 1.5 cm, while the charged areas are inserted within squares reaching as much as 3 cm each side. This shows that charges produced by even short-lasting friction quickly spread to areas adjacent to those where mechanical action actually took place. Few other smaller areas with charge excess are eventually observed, but the most often found pattern is a dipole formed by spread charges.

On the other hand, PE maps also show positive/negative domains or positive domains only. Nevertheless, the pixel potentials in the PE maps are much lower than in PTFE, showing that both positive and negative charges are preferentially deposited on PTFE.

Net charge on each sample can be calculated from the respective potential map by summing up the contributions made by every map pixel as described in a previous paper,[39] and it can also be directly determined using a Faraday cup. Results in Table 1 show that the two methods agree within 10% or better, which is very good considering the complete independence of the two procedures, the low spatial resolution of the potential measurements, and the fractal geometry of charge distribution. Moreover, this shows that potential maps account for all the charges incorporated in each sample.

Table 1. Net Charge Determined by Faraday Cup and by Summing up the Contributions Made by All Pixels in the Potential Maps Applying the Superposition Principle

materials	charge in Faraday cup/Coulomb	charge calculated by superposition principle/Coulomb
PTFE × PE foam	5.51×10^{-9}	6.01×10^{-9}
PMMA × PE foam	6.78×10^{-9}	6.61×10^{-9}
PE film × glass balls	-3.25×10^{-8}	-3.07×10^{-8}

Sequentially recording electrostatic potential maps from the same sample and plotting the potential of any given pixel as a function of time allows an assessment of the stability of charge patterns. A typical result is presented in Figure 2, showing that local potentials are rather stable. Plots for pixels well within each domain do not show significant variations, while those in borderline areas show noise that is probably due to deviations in positioning the scanning electrode. Only one pixel showed a definite trend of potential decrease, and this is tentatively assigned to nonuniformity of the contributing charged species, which means some charge-bearing species may lose charge to the atmosphere or to surrounding areas faster than others. Measured decrease in potential can also be due to charge penetration in the sample, because then the contribution to electrode potential would decrease. Considering all the data in Figure 2, charge penetration in PTFE is negligible in the present time scale but it can be faster in one or another area, due to the presence of pores or some other sample defect.

dx.doi.org/10.1021/la301228j | *Langmuir* 2012, 28, 7407−7416

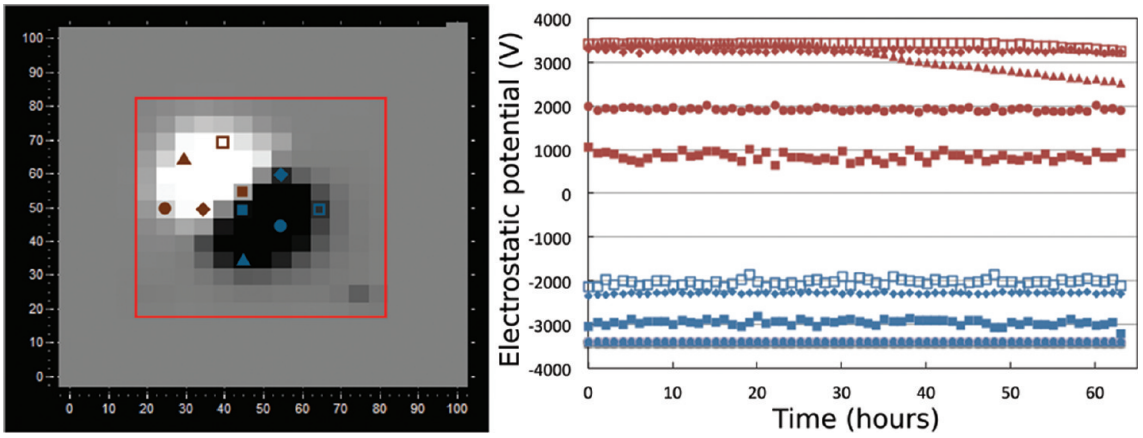

Figure 2. Electrostatic potential variation on PTFE tribocharged with PE foam. (Left) Potential pattern on PTFE abraded with PE foam. (Right) Electrostatic potential of the selected pixels measured during 63 h at 60% relative humidity. Negative potential is stable in every pixel, while some pixels with positive potential show a decrease with time.

Tribocharges are largely removed by immersion of the charged samples in liquids, as shown by the results in Figure 3. The ability of different liquids to abate charge varies significantly: ethanol is rather effective, more than water, aqueous NaCl solution, or *n*-hexane. The latter is much more effective to reduce positive than negative charge, while exposure of a PTFE tribocharged surface to a jet of 1,1-difluoroethane liquid at its −25 °C boiling point effectively removes positive and negative charges (Supporting Information Figure S2), similar to ethanol. However, the potential map of tribocharged PTFE exposed to a jet of difluoroethane vapor at room temperature does not change significantly.

Tribocharge removal by exposure to liquids may be due to many types of events: (a) extraction of ionic short polymer segments formed following polymer chain breakdown; (b) tribo-ions of opposite charge are allowed to migrate and they recombine forming block copolymer chains; (c) in the case of liquid water and other liquids with acid−base properties, ions like $[H^+(H_2O)_n]$ or $[OH^-(H_2O)_n]$ bind to polymer fragment ions, neutralizing their charge.

Free electrons may also be produced as transient species, when trapped ions are allowed to sample new environments or when they are allowed to migrate. Indeed, when groups of ions with opposite charge approach each other, at some critical distance they produce electric fields large enough to cause ionization of neutral molecules, producing electrons that were previously described in the literature.[11−17]

One interesting feature of the effect of water on positive domains on PTFE is the residual negative charge, after immersion in water. This is tentatively explained using the following assumption: the net positive domains also contain a significant but minute amount of negative ions that are not extracted together with the hydrocarbon cations. Another evidence for selective extraction is the enhanced effect of NaCl solution as compared to water: the solubility of sparingly soluble organic ions is often higher in salt solutions than in plain water.

A smoother PTFE surface, obtained by compression of PTFE film between two sheets of mica at 200 °C for 12 h (Supporting Information Figure S3), was also tribocharged with PE foam. Macroscopic positive and negative charge domains similar to those on "rougher" PTFE were observed. Rinsing the surface with water also removed the majority of the positive and negative charges.

Positive identification of charged species was done by using different techniques and the results obtained are presented in Figure 4. ATR/IR spectra (Figure 4a) from positive domains cut out from tribocharged PTFE show the existence of compounds with C−H bonds, but these are not observed in the negative areas, thus verifying that tribocations derive from PE.

Moreover, positive tribocharged domains on PTFE undergo discoloration upon heating, acquiring first a yellowish color that is followed by the appearance of dark spots that are shown in Figure 4b (right) and finally disappear upon further heating. This behavior is expected for PE charring and oxidation, but PTFE does not char, confirming that the positive macrodomains on PTFE are formed by species derived from PE. Negative domains on PTFE do not show any visible changes as expected considering that PTFE just depolymerizes upon heating, forming the volatile C_2F_4.

Positive identification of the constituent of negative domains formed on PTFE was achieved by extracting the negative tribocharged film with ethanol, transferring the liquid to an evaporated carbon film supported on a microscope grid and drying under air, followed by examination in an analytical transmission electron microscope fitted with an electron spectrometer. A set of micrographs of the dry extract is in Figure 5 showing that the extracted negative species contain fluorine and oxygen besides carbon and they are thus derived from PTFE. The effectiveness of charge extraction in ethanol and 1,1-difluoroethane can then be understood considering that the both have low solubility (Hildebrand) parameters and significant dipole moments. They should, therefore, be good solvents for both hydrocarbon and fluorocarbon ions.

To understand charge formation and segregation, we recall that, when two polymer surfaces are brought into contact, van der Waals attractive interactions develop through the outermost parts of the surfaces but not evenly, due to roughness. Mechanical action shearing the polymer−polymer interface is actually concentrated on a fraction of the overall area due to surface roughness, creating hot spots under large temperature and shear gradients, where the polymer is plasticized and/or molten. In the cases of similar or miscible polymers, chain entanglement[42] may develop through reptation,[43] but in most cases, polymers are immiscible and the sheared viscous polymer masses are kept separated, as expected from Flory−Huggins theory[44] and extensive experimental data on polymer−polymer

dx.doi.org/10.1021/la301228j | *Langmuir* 2012, 28, 7407−7416

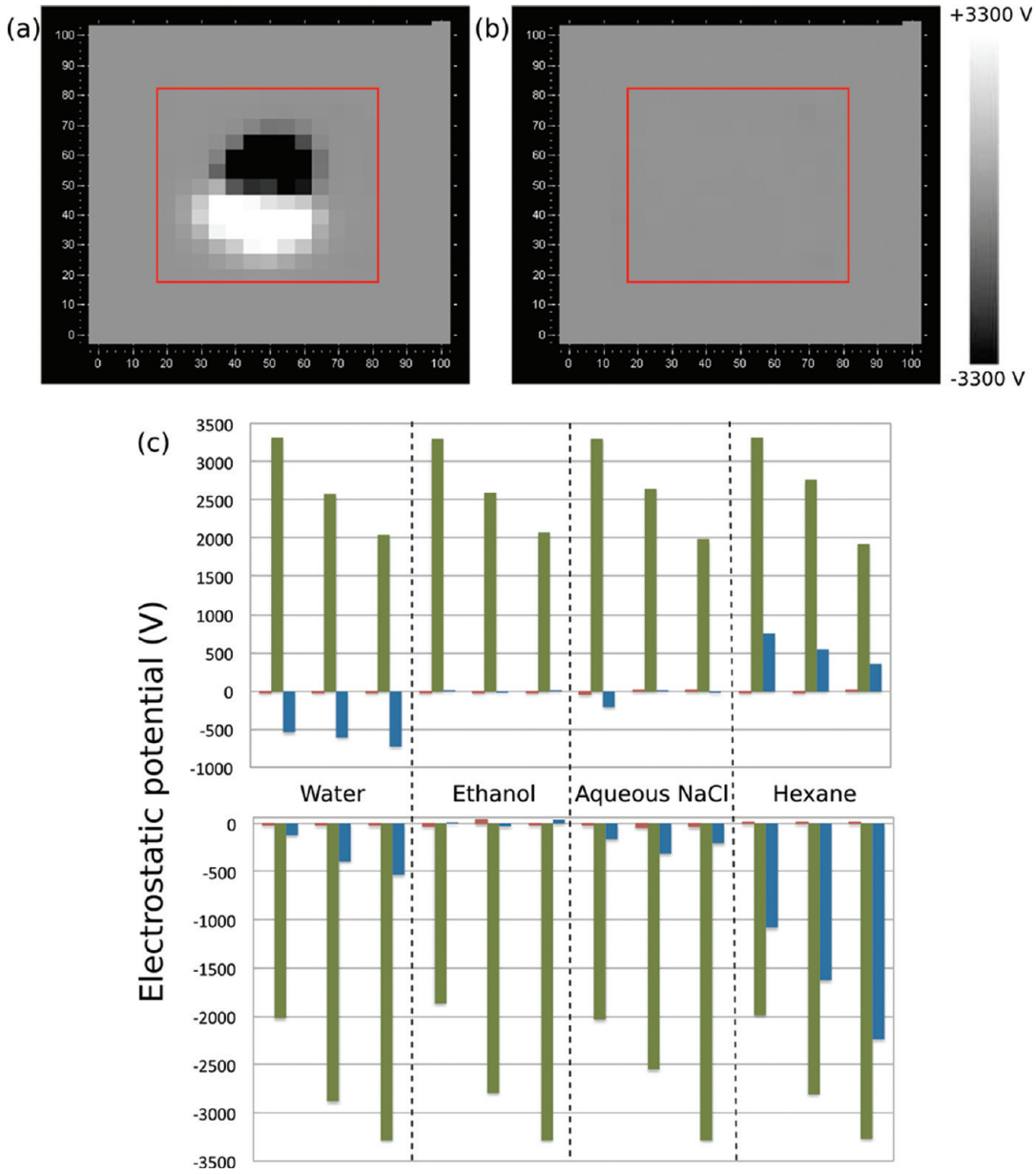

Figure 3. Charge elimination on PTFE using different liquids. Potential map in (a) PTFE after tribocharging with PE foam and (b) following immersion in ethanol for 2 h and drying under air. (c) Effect of solvents on the electric potential of six different areas (three positive, three negative) of PTFE tribocharged with PE foam. The electric potential on PTFE was measured before tribocharging (red bars), right after tribocharging with PE foam (green), and after washing with each liquid (blue).

miscibility. Partial mixing may also take place but only involving oligomer fractions and eventual contaminants.

There is always material transfer among two contacting polymer surfaces,[45,46] as well as under mild polymer−metal contact conditions.[47] This is facilitated when the polymer surfaces are covered with weakly bound layers (WBLs)[48,49] that are fairly universal and are formed by oligomers, misfit polymer chains, and impurities that are less dependent on the restrictions imposed by Flory−Huggins theory. On the other hand, material transfer among surfaces and its deposition on any surface is directed by the balance of relevant interfacial and surface tensions: interfacial areas with low interfacial tension tend to grow at the expense of the areas with higher surface tension.[50,51]

Mutual friction of the contacting surfaces increases the contact area and it forces one polymer to spread on top of the other under nonequilibrium conditions, even if the balance of interfacial forces mentioned in the previous paragraph is not favorable. Moreover, temperature peaks and high shear in the previously mentioned hot spots allow the formation of short-lived, highly unstable species, or triboplasma.[52−54] Extensive chain breakdown takes place, due to the combination of high temperature and mechanical pull of the entangled polymer chains.

Polymer chain breakdown can be heterolytic or homolytic.[55] In the former case, ionic chain-ends are formed, more or less fixed to the subsurface layers by the intact chain segments. Given the stochastic characteristics of electron distribution in ruptured chain bonds, equal amounts of positive and negative ions can be formed on both contacting surfaces, but only the most stable are expected to survive for longer periods.

dx.doi.org/10.1021/la301228j | *Langmuir* 2012, 28, 7407−7416

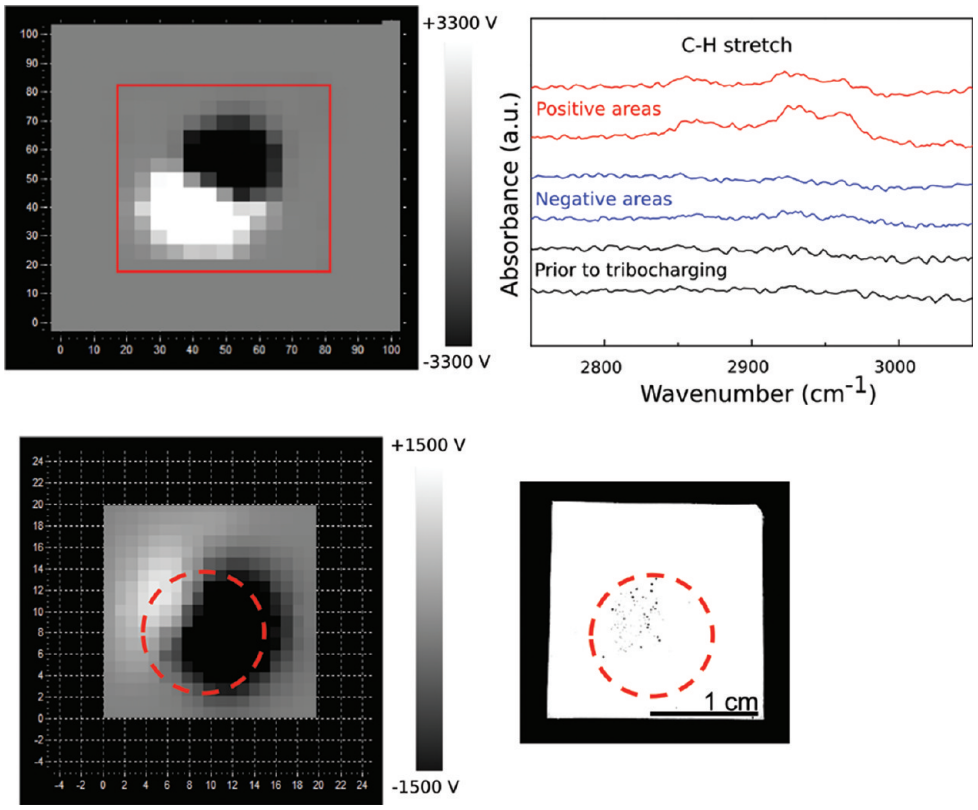

Figure 4. Left: potential maps of two pieces of PTFE charged by shearing with PE disk. Right: (a) IR reflectance spectra of positive and negative areas from the PTFE piece at left; (b) picture (contrast enhanced) of the PTFE piece mapped at left.

Both ions and free radicals formed by chain rupture are high-energy, unstable, short-lived species likely to enter a number of further reactions as, for instance, the well-known transformation of carbon radicals (R•) into peroxide radicals (ROO•)[56,57] under air, but these are not detected by charge measurements. In the case of PTFE rubbed with PE, the low polarity of carbon−carbon bonds in both polymer chains suggests that homolytic chain breakdown predominates. Further, electron transfer from hydrocarbon to fluorocarbon radicals is expected, following the higher electronegativity of the latter.[58,59]

This qualitative reasoning is supported by the calculation of Gibbs energies for the formation of positive and negative ions by electron transfer to and from fluorocarbon and hydrocarbon free radicals, shown in Table 2. Following these results, the formation of fluorocarbon anions from fluorocarbon free radicals is spontaneous but the formation of hydrocarbon anions and of both types of cations is not spontaneous. Nevertheless, hydrocarbon cation formation is more favorable than the formation of fluorocarbon cations, and the following redox reaction is the most likely to take place, involving free radicals formed tribochemically

$$-H_2CH_2CH_2C\cdot + -F_2CF_2CF_2C\cdot \rightarrow -H_2CH_2CH_2C^+ + -F_2CF_2CF_2C^-$$

The formation of the macroscopic charged domains is thus assigned to the accumulation of hydrocarbocations and fluorocarbanions, but these species are not expected to be stable under ambient conditions used in these experiments unless they are somehow chemically protected. Indeed, ions formed from polymer chain rupture are amphiphilic; this means the charge located at chain-ends creates a polar environment that tends to self-array at any interface with air, hiding the charged portion of the ion under a layer of unreacted polymer and thus protecting it from atmospheric water, oxygen, and other reactive substances. Thus, unstable species are trapped or occluded by stable, intact chain segments and chain ends that make a lower contribution to surface tension than the high-energy species.[50,51] The observation of large nonzero positive or negative potential and its slow decay[39] in PE was recently reported but using corona charging devices.

A mechanism for contact and triboelectrification of insulating polymers is schematically represented in Figure 6. The relative importance of the various events that can take place depends on the materials used, the history of their surfaces and subsurfaces, their morphology and oxidation state, the kinds of intervening mechanical actions, and the environment. For this reason, the outcome of the contact or friction between two surfaces should be spatially nonuniform,[60] creating electrostatic nanopatterns similar to those previously described in the literature[28−30,32] and the macroscopic patterns described in the present paper. Following the present results, the complex and stable electric patterns obtained by simple contact or friction of dielectric solids are necessarily dependent on highly fixed and stable charges, since the charge maps do not show significant modifications between successive scans, even across potential gradients as large as 6 MV/m, as, for instance, across the separation lines between positive and negative islands in Figure 1. These conditions are met by the hydrocarbon and fluorocarbon ionic species derived from macromolecules experimentally evidenced in this work.

The formation of large domains with excess positive or negative charge, in the case of the PTFE/PE pair, was not

dx.doi.org/10.1021/la301228j | *Langmuir* 2012, 28, 7407−7416

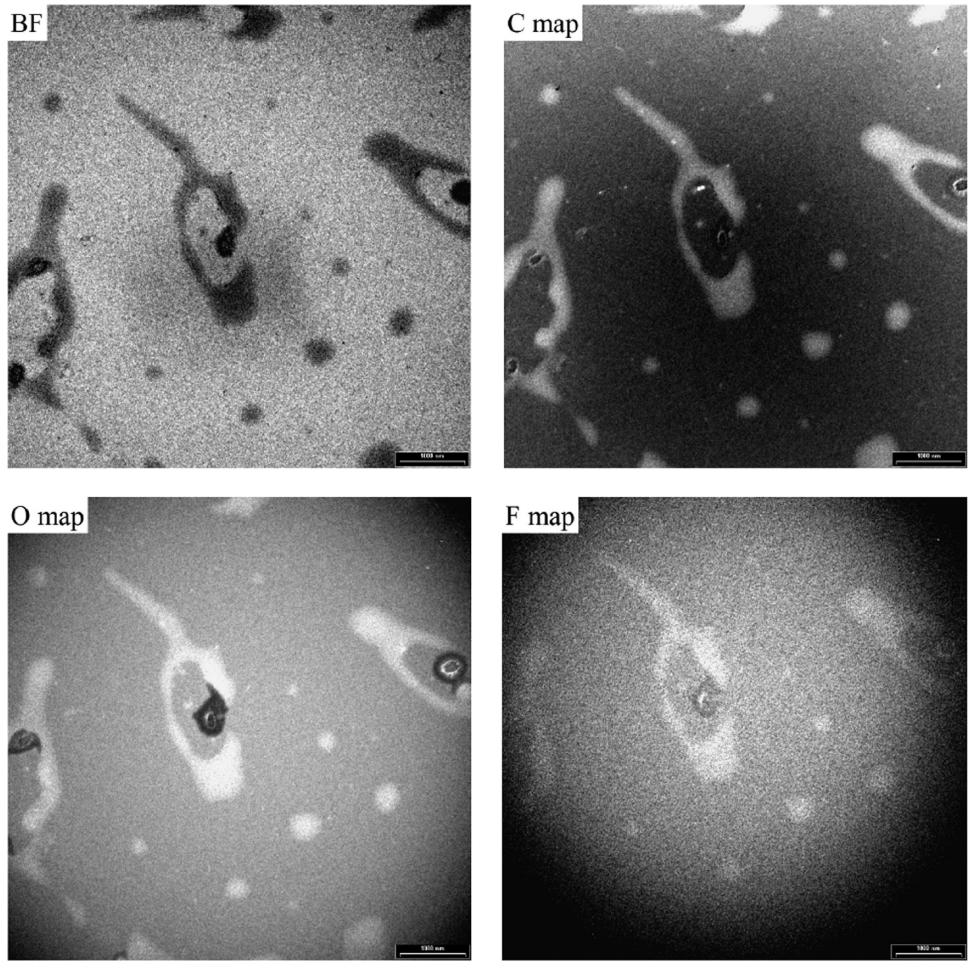

Figure 5. Bright field image (BF), carbon map (C map), oxygen map (O map), and fluorine map (F map) of the dry extract of the PTFE tribocharged surface.

Table 2. ΔG for the Formation of Ions from the Corresponding Hydrocarbon and Fluorocarbon Radicals

species formed	species charge	ΔG/(kJ/mol)
$CH_3(CH_2)_8CH_2^-$	−1	9.43
$CH_3(CH_2)_8CH_2^+$	+1	627.51
$CF_3(CF_2)_8CF_2^-$	−1	−216.91
$CF_3(CF_2)_8CF_2^+$	+1	902.16

previously demonstrated or even hinted at but it could have been predicted, considering current knowledge on polymer chain mechanochemistry and on the widespread polymer immiscibility[44] that counters electrostatic repulsion. This also explains why charge or potential nanopatterns have been found in any polymer surface that was previously examined: simple handling and contact of surfaces that are not atomically smooth concentrates mechanical energy in protruding areas, thus triggering a host of mechanochemical events followed by product segregation.

Using the techniques for charge build-up and dissipation described in this paper, we can make macroscopic electrostatic lithography on plain PTFE sheets, as shown in Figure 7.

Finally, we can now easily understand the great difficulty in establishing a tribochemical series that is abundantly described in the literature, because polymer tribocharging depends not only on a complex series of chemical events, but also on surface characteristics that were hardly accounted for, like surface roughness down to the atomic size range. The simple but effective model for tribocharging described in this work will certainly speed up the development of functional tribocharged materials and devices.

To sum up, electrostatic charge patterns deriving from contact and tribocharging events are presented here for the first time with a model to explain their appearance, based on their stability and on the effect of simple liquids, together with well-established knowledge on polymer surface behavior and polymer chemistry.

■ CONCLUSIONS

Polymer tribocharging produces macroscopic charge mosaics presenting large islands carrying either positive or negative net charge, including macroscopic electric dipoles. This confirms the fractal nature of electrostatic patterns on polymer surfaces, previously observed using scanning electric probe microscopy techniques. Tribocharges are identified for the first time, using suitably sensitive techniques, as polymer ions formed by polymer chain scission followed by electron transfer according to the polymer chain electronegativity, e.g., fluorinated alkyl residues acquire predominantly negative charge, while alkyl residues are predominantly positive. Cation and anion chain fragments further segregate according to their chemical nature, following Flory−Huggins theory and thus forming the charge islands.

dx.doi.org/10.1021/la301228j | *Langmuir* 2012, 28, 7407−7416

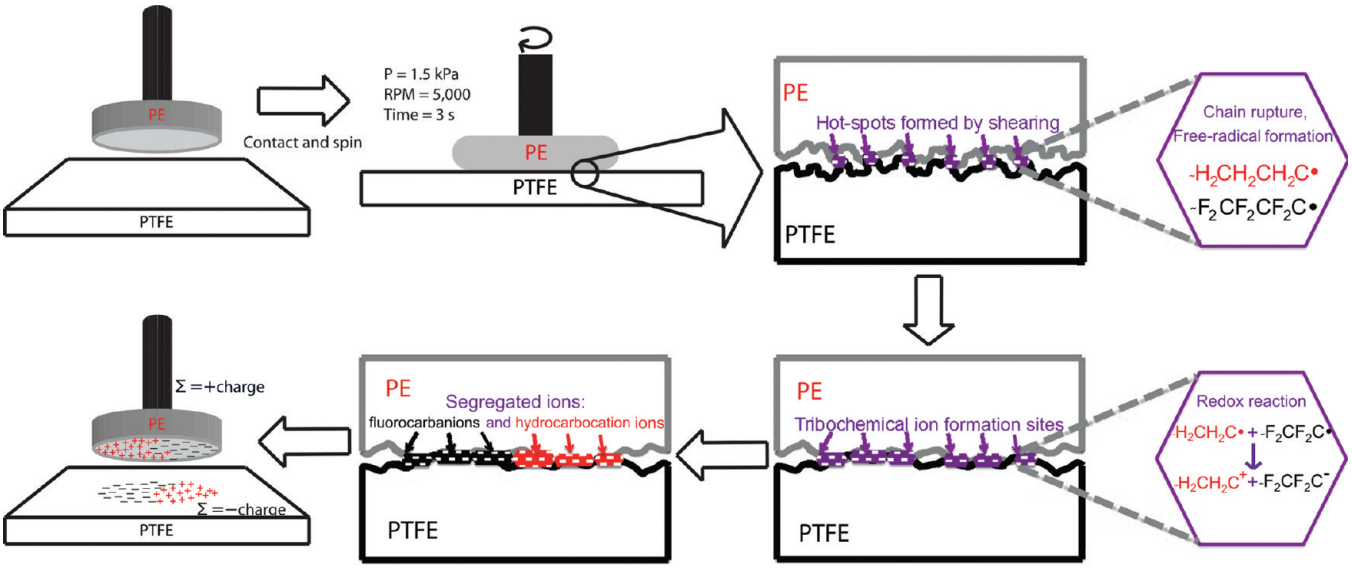

Figure 6. Mechanism for contact triboelectrification of insulating polymers. Shearing the polymer interface heats both surfaces unevenly forming hot spots, due to forced contact on surface hills. Plasticization and melting take place, added to chain breakdown and fragmentation. Homolytic scission produces free radicals with markedly different electronegativities that are converted into fluorocarbanions and hydrocarbocations by electron transfer. Ions are segregated due to the chain size, following Flory–Huggins theory and superseding weak electrostatic interactions between highly spaced charges.

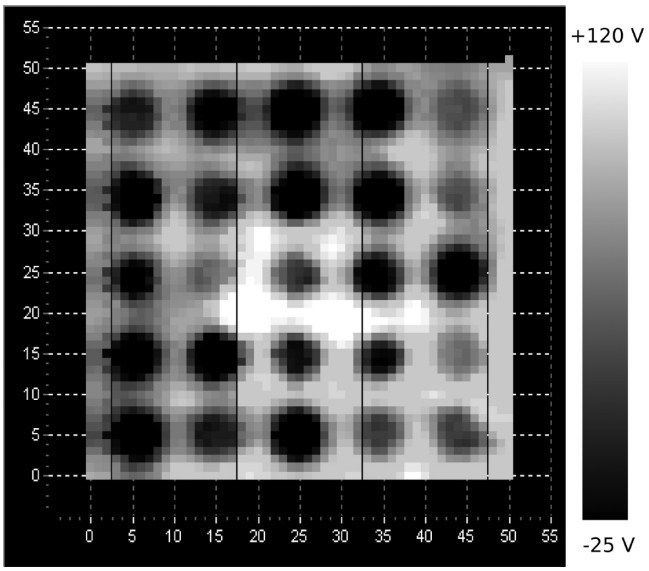

Figure 7. Macroscopic patterns obtained on PTFE surface. An aluminum sheet mask with drilled circular holes was mounted on top of spacers, 1 mm above the PTFE surface. 2-mm-diameter washed glass spheres were placed on each hole and the whole setup was shaken on a reciprocating platform for 60 min, after which the PTFE was placed on the *x*–*y* scanner for potential mapping.

Tribocharge is extracted with both nonpolar and polar liquids but shows some solvent specificity, and the analysis of the extracts by analytical TEM confirms that fluorocarbanions are the negative tribocharge species. Charge stability at the polymer surfaces under air is explained by the tendency of ions bound to apolar chains to occupy subsurface layers, to minimize surface tension.

Positive and negative domains can be cut and mounted, and they can be produced forming regular patterns, as a new and simple potential alternative for electrolithography.

■ ASSOCIATED CONTENT

Supporting Information

Electric potential maps of PTFE and PE samples. Removal of charges from tribocharged PTFE by 1,1-difluoroethane. Electrostatic potential maps of PTFE pressed between cleaved mica sheets. Complete ref 41. This material is available free of charge via the Internet at http://pubs.acs.org.

■ AUTHOR INFORMATION

Corresponding Author

*E-mail: fernagal@iqm.unicamp.br.

Notes

The authors declare no competing financial interest.

■ ACKNOWLEDGMENTS

Supported by CNPq and Fapesp (Brazil) through Inomat, National Institute (INCT) for Complex Functional Materials. T.A.L.B., T.R.D.D., and K.J.C. hold fellowships from CNPq, and K.R.F. holds a fellowship from Fapesp.

■ REFERENCES

(1) Crowley, J. M. *Fundamentals of Applied Electrostatics*; Wiley: New York, 1986.
(2) Bailey, A. G. The Charging of insulator surfaces. *J. Electrostat.* **2001**, *51*–*52*, 82–90.
(3) Harper, W. R. *Contact and Frictional Electrification*; Laplacian: Morgan Hill, 1998.
(4) Castle, G. S. P. Contact charging between insulators. *J. Electrostat.* **1997**, *40*, 13–20.
(5) Schein, L. B. Recent progress and continuing puzzles in electrostatics. *Science* **2007**, *316*, 1572–1573.
(6) Loeb, L. B. The basic mechanisms of static electrification. *Science* **1945**, *102*, 573–576.
(7) Williams, M. W. Triboelectric charging of insulators – Evidence for electrons versus ions. *IEEE Trans. Ind. Appl.* **2011**, *47*, 1093–1099.
(8) Matsusaka, S.; Maruyama, H.; Matsuyama, T.; Ghadiri, M. Triboelectric charging of powders: A review. *Chem. Eng. Sci.* **2010**, *65*, 5781–5807.

(9) Gibson, H. W.; Bailey, F. C.; Mincer, J. L.; Gunther, W. H. H. Chemical modification of polymers. 12. Control of triboelectric charging properties of polymers by chemical modification. *J. Polym. Sci., Polym. Chem. Ed.* **1979**, *17*, 2961−2974.
(10) Friedle, S.; Thomas, S. W., III. Controlling contact electrification with photochromic polymers. *Angew. Chem., Int. Ed.* **2010**, *49*, 7968−7971.
(11) Liu, C. Y.; Bard, A. J. Electrostatic electrochemistry at insulators. *Nat. Mater.* **2008**, *7*, 505−509.
(12) Liu, C. Y.; Bard, A. J. Chemical redox reactions induced by cryptoelectrons on a PMMA surface. *J. Am. Chem. Soc.* **2009**, *131*, 6397−6401.
(13) Grzybowski, B. A.; Fialkowski, M.; Wiles, J. A. Kinetics of contact electrification between metals and polymers. *J. Phys. Chem. B* **2005**, *109*, 20511−20515.
(14) Lowell, J.; Rose-Innes, A. C. Contact electrification. *Adv. Phys.* **1980**, *29*, 947−1023.
(15) Gibson, H. W. Linear free energy relationships. 5. Triboelectric charging of organic solids. *J. Am. Chem. Soc.* **1975**, *97*, 3832−3833.
(16) Gibson, H. W.; Bailey, F. C. Linear free-energy relationships - Triboelectric charging of poly(olefins). *Chem. Phys. Lett.* **1977**, *51*, 352−355.
(17) Gibson, H. W. in *Modification of Polymers*, Carraher, C. E., , Jr., Moore, J. A., Eds.; Plenum Publishing Corporation: New York, 1983; pp 353−372.
(18) Diaz, A. F.; Wollmann, D.; Dreblow, D. Contact Electrification: Ion transfer to metals and polymers. *Chem. Mater.* **1991**, *3*, 997−999.
(19) McCarty, L. S.; Winkleman, A.; Whitesides, G. M. Ionic electrets: Electrostatic charging of surfaces by transferring mobile ions upon contact. *J. Am. Chem. Soc.* **2007**, *129*, 4075−4088.
(20) Diaz, A. F.; Guay, J. Contact charging of organic materials − Ion vs electron-transfer. *IBM J. Res. Dev.* **1993**, *37*, 249−259.
(21) Davies, D. K. Charge generation of dielectric surfaces. *J. Phys. D: Appl. Phys.* **1969**, *2*, 1533−1537.
(22) Duke, C. B.; Fabish, T. J. Contact electrification of polymers: A quantitative model. *J. Appl. Phys.* **1978**, *49*, 315−321.
(23) Jacobs, H. O.; Knapp, H. F.; Stemmer, A. Surface potential mapping: A qualitative material contrast in SPM. *Ultramicroscopy* **1997**, *69*, 39−49.
(24) Gouveia, R. F.; Galembeck, F. Electrostatic charging of hydrophilic particles due to water adsorption. *J. Am. Chem. Soc.* **2009**, *131*, 11381−11386.
(25) Gouveia, R. F.; Costa, C. A. R.; Galembeck, F. Water vapor adsorption effect on sílica surface electrostatic patterning. *J. Phys. Chem. C* **2008**, *112*, 17193−17199.
(26) Gouveia, R. F.; Costa, C. A. R.; Galembeck, F. Electrostatic patterning of a sílica surface: A new model for charge build-up on a dielectric solid. *J. Phys. Chem. B* **2005**, *109*, 4631−4637.
(27) Diaz, A. F.; Felix-Navarro, R. M. A semi-quantitative tribo-electric series for polymeric materials: the influence of chemical structure and properties. *J. Electrostat.* **2004**, *62*, 277−290.
(28) Baytekin, H. T.; Patashinski, A. Z.; Branicki, M.; Baytekin, B.; Soh, S.; Grzybowski, B. A. The mosaic of surface charge in contact electrification. *Science* **2011**, *333*, 308−312.
(29) Terris, B. D.; Stern, J. E.; Rugar, D.; Mamin, H. J. Contact electrification using force microscopy. *Phys. Rev. Lett.* **1989**, *63*, 2669−2672.
(30) Knorr, N. Squeezing out hydrated protons: low-frictional-energy triboelectric insulator charging on a microscopic scale. *AIP Advances* **2011**, *1*, 022119.
(31) Grzybowski, B. A.; Winkleman, A.; Wiles, J. A.; Brumer, Y.; Whitesides, G. M. Electrostatic self-assembly of macroscopic crystals using contact electrification. *Nat. Mater.* **2003**, *2*, 241−245.
(32) Galembeck, A.; Costa, C. A. R.; Silva, M. C. V. M; Souza, E. F.; Galembeck, F. Scanning electric potential microscopy imaging of polymers: electrical charge distribution in dielectrics. *Polymer* **2001**, *42*, 4845−4851.
(33) Braga, M.; Costa, C. A. R.; Leite, C. A. P.; Galembeck, F. Scanning electric potential microscopy imaging of polymer latex films: Detection of supramolecular domains with nonuniform electrical characteristics. *J. Phys. Chem. B* **2001**, *105*, 3005−3011.
(34) Soares, L. C.; Bertazzo, S.; Burgo, T. A. L.; Baldim, V.; Galembeck, F. A new mechanism for the electrostatic charge build-up and dissipation in dielectrics. *J. Braz. Chem. Soc.* **2008**, *19*, 277−286.
(35) Bernardes, J. S.; Rezende, C. A.; Galembeck, F. Electrostatic patterns on surfactant coatings change with ambient humidity. *J. Phys. Chem. C* **2010**, *114*, 19016−19023.
(36) Ducati, T. R. D.; Simões, L. H.; Galembeck, F. Charge partitioning at gas − solid interfaces: Humidity causes electricity buildup on metals. *Langmuir* **2010**, *26*, 13763−13766.
(37) Healy, T. W; Fuerstenau, D. W. The isoelectric point/point-of zero-charge of interfaces formed by aqueous solutions and nonpolar solids, liquids, and gases. *J. Colloid Interface Sci.* **2007**, *309*, 183−188.
(38) Creux, P.; Lachaise, J.; Graciaa, A.; Beattie, J. K.; Djerdjev, A. M. Strong specific hydroxide ion binding at the pristine oil/water and air/water interfaces. *J. Phys. Chem. B* **2009**, *113*, 14146−14150.
(39) Burgo, T. A. L.; Rezende, C. A.; Bertazzo, S.; Galembeck, A.; Galembeck, F. Electric potential decay on polyethylene: Role of atmospheric water on electric charge build-up and dissipation. *J. Electrostat.* **2011**, *69*, 401−409.
(40) Santos, L. P.; Ducati, T. R. D.; Balestrin, L. B. S.; Galembeck, F. Water with excess electric charge. *J. Phys. Chem. C* **2011**, *115*, 11226−11232.
(41) *Gaussian 09*, revision A.02; Frisch, M. J. et al. Gaussian, Inc., Wallingford, CT, 2009.
(42) DeGennes, P. G. *Scaling Concepts in Polymer Physics*; Cornell University Press: Ithaca, 1979; pp 219−240.
(43) DeGennes, P. G. Reptation of a polymer chain in the presence of fixed obstacles. *J. Chem. Phys.* **1971**, *55*, 572−579.
(44) Elias, H. G. *Macromolecules*; Plenum Press: New York, 1984; pp 213−216.
(45) Gong, D.; Xue, Q.; Wang, H. ESCA study on tribochemical characteristics of filled PTFE. *Wear* **1991**, *148*, 161−169.
(46) Lu, X.; Wong, K. C.; Wong, P. C.; Mitchell, K. A. R.; Cotter, J.; Eadie, D. T. Surface characterization of polytetrafluoroethylene (PTFE) transfer films during rolling-sliding tribology tests using X-ray photoelectron spectroscopy. *Wear* **2006**, *261*, 1155−1162.
(47) Gibson, H. W.; Pochan, J. M.; Bailey, F. C. Surface analyses by a triboelectric charging technique. *Anal. Chem.* **1979**, *51*, 483−487.
(48) Mittal, K. L. Adhesion aspects of metallization of organic polymer surfaces. *J. Vac. Sci. Technol.* **1976**, *13*, 19−25.
(49) Good, R. J. Theory of cohesive vs adhesive separation in an adhering system. *J. Adhes.* **1972**, *4*, 133−154.
(50) Leclercq, B.; Sotton, M.; Baszkin, A.; Ter-Minassian-Saraga, L. Surface modification of corona treated poly(ethylene terephthalate) film: adsorption and wettability studies. *Polymer* **1977**, *18*, 675−680.
(51) Adam, N. K. *The Physics and Chemistry of Surfaces*, 3rd ed.; Oxford University Press: London, 1941.
(52) Heinicke, G. *Tribochemistry*; Carl Hanser: Berlin, 1984.
(53) Dascalescu, D.; Polychronopoulou, K.; Polycarpou, A. A. The significance of tribochemistry on the performance of PTFE-based coatings in CO_2 refrigerant environment. *Surf. Coat. Technol.* **2009**, *204*, 319−329.
(54) Kajdas, C. K. Importance of the triboemission process for tribochemical reaction. *Tribol. Int.* **2005**, *38*, 337−353.
(55) Caruso, M. M.; Davis, D. A.; Shen, Q.; Odom, S. A.; Sottos, N. R.; White, S. R.; Moore, J. S. Mechanically-induced chemical changes in polymeric materials. *Chem. Rev.* **2009**, *109*, 5755−5798.
(56) Allayarov, S. R.; Konovalova, T. A.; Waterfield, A.; Focsan, A. L.; Jackson, V.; Craciun, R.; Kispert, L. D.; Thrasher, J. S.; Dixon, D. A. Low-temperature fluorination of fluoro-containing polymers EPR studies of polyvinylidenefluoride and the copolymer of tetrafluoro-ethylene with ethylene. *J. Fluorine Chem.* **2006**, *127*, 1294−1301.
(57) Oshima, A.; Seguchi, T.; Tabata, Y. ESR study on free radicals trapped in crosslinked polytetrafluoroethylene (PTFE) − II radical formation and reactivity. *Radiat. Phys. Chem.* **1999**, *55*, 61−71.
(58) Huheey, J. E. The electronegativity of groups. *J. Phys. Chem.* **1965**, *69*, 3284−3291.

(59) Dolbier, W. R. Structure, reactivity, and chemistry of fluoroalkyl radicals. *Chem. Rev.* **1996**, *96*, 1557−1584.
(60) Baytekin, H. T.; Baytekin, B.; Incorvati, J. T.; Grzybowski., B. A. Material transfer and polarity reversal in contact charging. *Angew. Chem., Int. Ed.* **2012**, DOI: 10.1002/anie.201200057.